JOURNAL OF APPLIED POLYMER SCIENCE VOL. 17, PP. 1715–1725 (1973)

Studies on Biaxial Stretching of Polypropylene Film. IX. Melting Behavior of Biaxially Stretched Film in One Step

HIROSHI TANAKA, TORU MASUKO, and SABURO OKAJIMA,*
Faculty of Technology, Tokyo Metropolitan University, Setagaya-ku, Tokyo, Japan

Synopsis

Melting temperature of a film biaxially stretched in one step in air at 152 or 140°C increases with increase of v_A, whereas heat of fusion and density decrease with increase of v_A, where v_A is the degree of stretching in area. The rapid decrease in density occurs for $v_A > 10$. Extrapolation of the plot of the density versus $v_A^{-1/2}$ gives a value of 0.870 g/cm^3 at infinite v_A, which has been reported as the amorphous density of isotactic polypropylene by Farrow. This is so because the fine structure of the film becomes more and more amorphous with further stretching and reaches completely amorphous state at infinite v_A. The temperature of stretching has a strong effect on the thermal behavior of a film; a low stretching temperature (140°C) brings about lower melting temperature, heat of fusion, and density. Crystallinity after melt press has not so large an effect on the melting behavior as the stretching temperature. Melting temperature and the shape of the thermogram also depend on the heating rate. There is an appropriate heating rate depending on v_A which gives the minimum melting temperature. With stretched samples, a small side peak or a shoulder appears at a relatively low temperature in the thermogram when a high heating rate is used.

INTRODUCTION

Relatively many papers concerning the thermal characteristics of isotactic polypropylene, such as equilibrium melting temperature[1–7] and heat of fusion,[3,5,8–13] have been published. The melting behavior of unstretched isotactic polypropylene treated thermally in various ways has also been reported,[4,6,7,14–18] but only a few papers describe the stretching effect on the melting behavior of isotactic polypropylene films and fibers.[1,19–21] The method of stretching adopted so far has been mainly uniaxial cold-drawing and not biaxial stretching. Therefore, it is interesting and meaningful to study the relation between the melting behavior and the orientation of molecules caused by the stretching, especially by biaxial stretching. In this paper, the isotactic polypropylene films biaxially stretched in one step in air at high temperatures are investigated, and a discussion is presented

* Present address: Faculty of Engineering, Yamagata University, Yonezawa, Yamagata-ken, Japan.

in conjunction with the deformation mechanism reported in a preceding paper.[22]

EXPERIMENTAL

Sample Films

The characteristics of the sample films used in this study are listed in Table I. Film B_5 was used unless specially noted.

TABLE I
Characteristics of Sample Films

Sample film[a]	$\bar{M}_v$[b]	Isotacticity, %[c]	Thickness, μ
B_5	2.5×10^5	94	350
B_6	2.9×10^5	96	850

[a] The sample films used were commercial films denoted by B in our laboratory; subscript indicates lot number.

[b] Evaluated by the equation of Kinsinger and Hughes.[23]

[c] Determined by extraction with boiling n-heptane.

Preparation of Films

A piece of B_5 or B_6 was melt-pressed at 230°C for 5 min at a pressure of 5 kg/cm^2 between chrome-plated iron plates 0.5 mm in thickness and cooled in ice water or boiling water for 5 min to obtain films with different crystallinities. The crystallinities calculated by the density method using the values of 0.936 g/cm^3 as the crystal density and 0.870 g/cm^3 as the amorphous density[24] were 25% and 52% for B_5 films cooled in ice water and in boiling water, respectively, and 32% for B_6 film cooled in ice water. The density of a film was calculated from the relation between the refractive index and the density which had been reported in a previous paper.[25]

Stretching

A piece of film 12 × 12 cm was mounted on an apparatus[26] and biaxially stretched in one step in air at 152°C or 140°C at a rate of about 4 mm/sec. The film was always stretched in equal amounts in two mutually perpendicular directions. Immediately after the stretching, the sample was

TABLE II
Four Kinds of Sample

Sample no.	Sample film	Crystallinity of melt-pressed film, %	Stretching temp., °C
1	B_5	25	152
2	B_5	25	140
3	B_5	52	152
4	B_6	32	152

detached from the apparatus and cooled to room temperature. Four kinds of samples were obtained from B_5 and B_6 by varying the cooling conditions after the melt press and subsequent stretching temperature (Table II).

Investigation of Melting Behavior

In order to investigate the melting behavior of the samples, a Perkin Elmer differential scanning calorimeter (DSC-1B) was employed. In this paper, the temperature of the main peak of the thermogram was denoted by T_{m2}, and that of the end of melting was denoted by T_{m3}. The heat of fusion was calculated from the area enclosed by the curve of the thermogram and the baseline and was denoted by ΔH. Purified benzoic acid was adopted as a standard substance for calibration, 33.9 cal/g being taken for its heat of fusion.

RESULTS AND DISCUSSION

Typical DSC thermograms of samples 1–3 in Table II are shown in Figure 1, which were obtained at a heating rate (HR) of 16°C/min. As is well known, it is necessary to use an appropriate HR to investigate the thermal properties of polymer samples through DSC. This is because

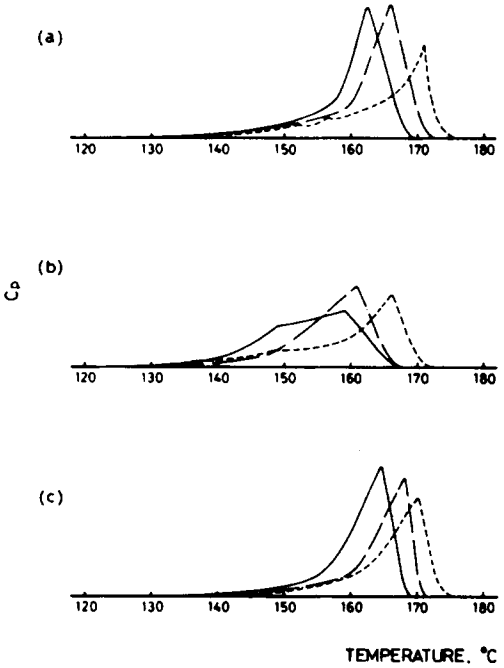

Fig. 1. Thermograms of samples 1, 2, and 3 in Table II; heating rate is 16°C/min. (a) sample 1: (——) v_A = 1.0 (unstretched, only preheated); (—·—) v_A = 2.3; (- - - -) v_A = 50. (b) sample 2: (——) v_A = 1.0 (unstretched, only preheated); (—·—) v_A = 2.3; (- - - -) v_A = 18. (c) sample 3: (——) v_A = 1.0 (unstretched, only preheated); (—·—) v_A = 8.4; (- - - -) v_A = 18.

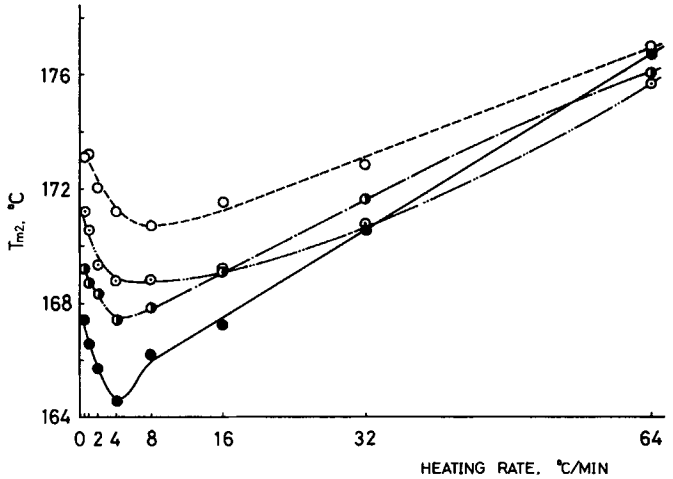

Fig. 2. Plot of T_{m2} versus heating rate, sample 4: (●) v_A = 1.0 (unstretched, only preheated); (◑) v_A = 4; (⊙) v_A = 10; (○) v_A = 20.

too slow HR brings about partial melting–recrystallization phenomena during the heating process, while too rapid HR brings about superheating, both of which are the main causes for higher T_{m2} or T_{m3}. It is also true that these behaviors are related to the fine structure of the sample, such as the thermal stability of crystallites and their distribution. Hence the effects of HR upon the DSC thermogram were studied by using film B_6; the effects observed in B_6 are believed to be true also of B_5.

Figure 2 represents the effect of HR on T_{m2} of the films stretched biaxially to various degrees. It is clearly seen that first T_{m2} drops and then rises, passing through a minimum as HR increases. The HR giving the lowest T_{m2} is about 4°C/min, and the HR has a tendency to shift slightly higher as v_A increases. In general, it is not an easy matter to find the optimum HR, causing neither partial melting–recrystallization nor superheating, which enables one to investigate the fine structure of samples directly. It is obvious that the employment of too slow or too rapid HR is not suitable for the purpose of this study. In this connection, the HR of 16°C/min employed in the following study is safe.

Figure 3 shows the thermograms of the samples with v_A = 1, 4, 10, and 20, which were measured by varying the HR at three levels, 0.5, 8, and 64°C/min. When the thermograms measured at HR = 0.5°C/min are compared with each other, it is clearly seen that the higher the degree of stretching, the sharper the thermogram is, and that T_{m2} becomes closer to T_{m3}. The cause of these changes is attributable to change in the thermal stability distribution of the crystallites, which was brought about by stretching. As already reported[22] and also mentioned below, the destruction of lamellar crystals into smaller blocks, the unfolding of chain molecules, and subsequent recrystallization into intermolecular crystals are conspicuous at v_A larger than 10. As the newly developed intermolecular crystallites are

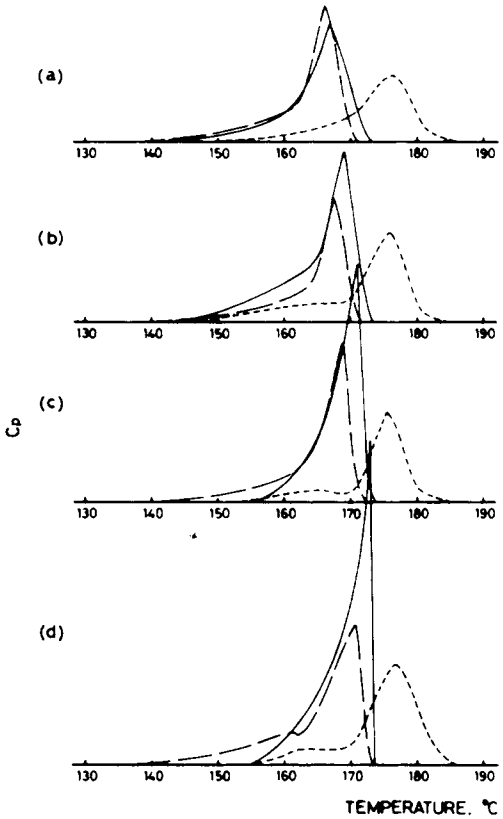

Fig. 3. Thermograms of sample 4 for various heating rates. (a) v_A = 1.0, heating rate: (——) 0.5°C/min; (—·—) 8°C/min; (- - - -) 64°C/min; (b) v_A = 4, heating rate: (——) 0.5°C/min; (—·—) 8°C/min; (- - - -) 64°C/min. (c) v_A = 10, heating rate: (——) 0.5°C/min; (—·—) 8°C/min; (- - - -) 64°C/min. (d) v_A = 20, heating rate: (——) 0.5°C/min; (—·—) 8°C/min; (- - - -) 64°C/min.

believed to have lower stability, the mode of the stability distribution of the highly stretched samples becomes broader at the lower-stability side (lower-temperature side) as v_A becomes larger. However, when HR is too small, less stable crystallites melt more easily and recrystallize into more stable ones during the heating process. Therefore, the thermogram with higher v_A becomes sharper, especially when v_A is larger than 10.

The thermograms obtained at HR = 64°C/min shift toward the higher-temperature side predominantly because of the dominant effect of superheating. Only a slight sharpening of the thermogram by stretching and long tailing toward the lower-temperature side for v_A = 1 and 4 are the result of suppressed premelting to a considerable extent. The appearance of a small peak at 160–170°C in Figures 3c and 3d suggests the distribution of crystallites newly yielded by stretching, the details of which are not clear. Taking the effect of superheating into consideration, the determination of the original distribution of crystallite stability only by controlling HR is

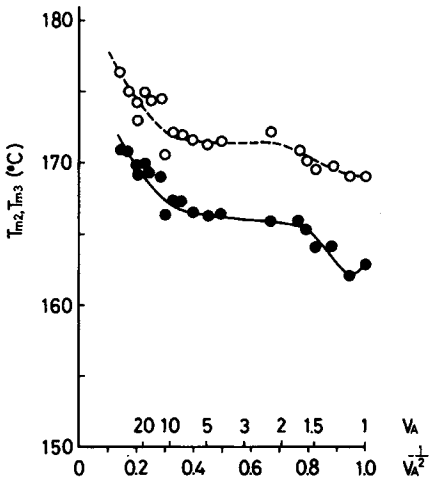

Fig. 4. Plots of T_{m2} and T_{m3} vs. $v_A^{-1/2}$ for sample 1: (●) T_{m2}; (○) T_{m3}.

very difficult. Therefore, we have to be content with the thermogram in which the original distribution of crystallites is reflected as closely as possible. The thermograms obtained at HR = 8°C/min seem to be between two thermograms obtained at HR = 0.5°C/min and 64°C/min.

We now return to Figure 1. Figure 1a is very similar to Figure 1c, but significantly different from Figure 1b, especially when $v_A = 1$. The differences of the fine structure induced by cooling at different temperatures are diminished to a great extent after preheating at the same temperature. This makes it possible that the subsequent stretching proceeds more or less in a similar way. The broader thermogram of sample 2 (Fig. 1b) and its lower T_{m2} are due to the lower stretching temperature compared with sample 1 (Fig. 1a). A quenched film crystallizes partially during preheating, and the distribution of the crystallite stability becomes sharper. The change is more eminent in the preheating at high temperatures. A previous microscopic study[28] indicates that the fragmentation of lamellae by stretching proceeds more heterogeneously at the lower temperature than at the higher temperature. These two effects yield a broader thermogram in Figure 1b.

Figure 4 shows the plots of T_{m2} and T_{m3} versus $v_A^{-1/2}$ for sample 1. T_{m2} and T_{m3} increase with increase in v_A, and T_{m2} changes approximately parallel with T_{m3}, except for a slight decrease at the initial stage of stretching. For larger v_A, however, T_{m2} and T_{m3} approach each other somewhat. The approach is probably due to the destruction of lamellae, which proceeds more significantly for crystallites having a melting point near T_{m2} than those having a melting point near T_{m3}, resulting in a decrease in peak height of the thermogram and the shifting of T_{m2} to T_{m3}.

It has already been reported by the authors[27] that the plot of $-\Delta n_{ss}$ versus $v_A^{-1/2}$ for a quenched film is composed of three intersecting lines with different slopes, from which region 1 ($v_A < 1.5$), region 2 ($1.5 < v_A < 10$), and

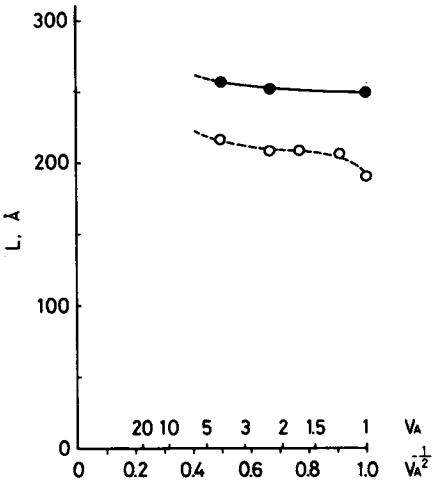

Fig. 5. Change in long period L obtained by small-angle x-ray scattering pattern during stretching: (●) sample 1 stretched at 152°C; (○) sample 2 stretched at 140°C.

region 3 ($v_A > 10$) were defined and deformation mechanisms for each of the three regions suggested.[22] Here, Δn_{ss} is the birefringence with respect to the normal to the film. In the preceding paper,[22] it was suggested that the increase in $-\Delta n_{ss}$ in region 1 is primarily attributable to the change in the orientation of the amorphous chains. A recent study, however, has shown that the change in the orientation of lamellae at the initial stage of stretching also contributes to the birefringence change to a certain extent. The details will be reported elsewhere.

Regions similar to those in the $-\Delta n_{ss}$ change also appear in the T_{m2} or T_{m3} plot. In view of the fact that in region 1 the $-\Delta n_{ss}$ increases considerably in spite of the very small change in density, the cause of the increase in T_{m2} in this region is attributable to the strain imposed on the tie molecules connecting the lamellae, inasmuch as the change in the orientation of the lamellae themselves is considered not to contribute to the increase in T_{m2}. The change of the long period L, obtained from small-angle x-ray scattering, is too small (Fig. 5) to explain the change in T_{m2}.

It has been suggested that the rotation and breaking of lamellae occur predominantly in region 2.[22] A slight decrease in density in this region (Fig. 8) is explained by the breaking of lamellae into small blocks. On the other hand, the strain imposed on the tie molecules becomes greater with increase in v_A. These factors affect T_{m2} concurrently, resulting in a relatively small increase in T_{m2}. At the same time, the partial melting and recrystallization which would occur during stretching seem to elevate T_{m2}.

In region 3, pulling of the chain molecules out of the crystallite fragments and subsequent recrystallization into intermolecular crystals are predominant.[22] Taking the dependence of the thermogram on HR (Fig. 3d) and the change in density (Fig. 8) into consideration, the development of large, stable crystallites is not plausible. Therefore, the rise in T_{m2} in this region

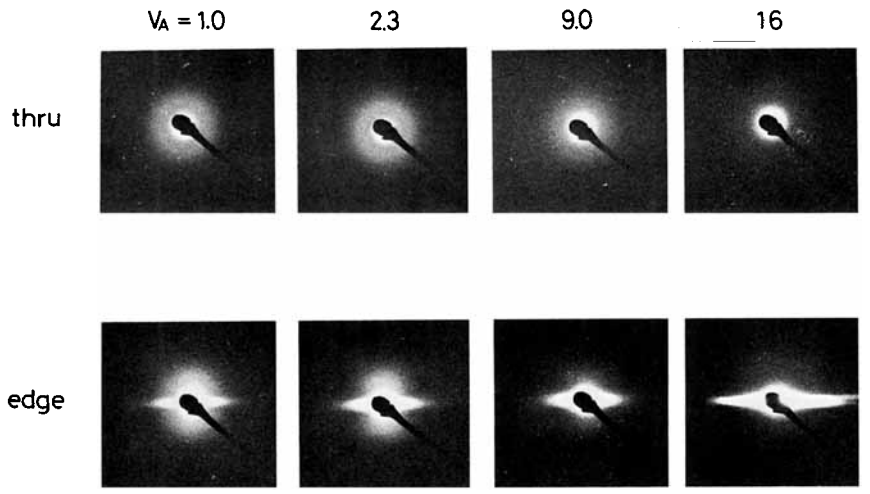

Fig. 6. Small-angle x-ray scattering pattern of sample 1 stretched to various degrees. Equatorial direction in the edge view corresponds with the direction normal to the film.

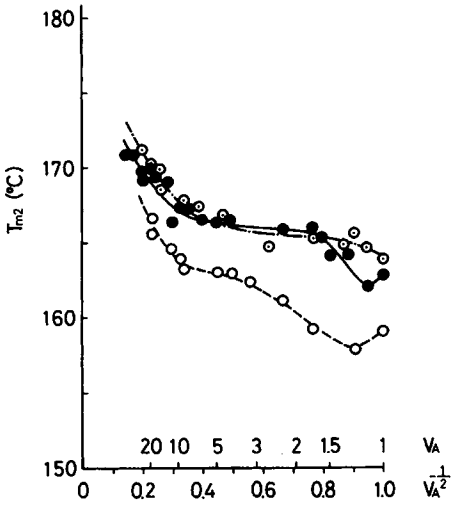

Fig. 7. Plot of T_{m2} vs. $v_A^{-1/2}$ for samples 1, 2, and 3: (●) sample 1; (○) sample 2; (⊙) sample 3.

would be mainly ascribed to the increased strain imposed on the molecular chains connecting the crystallites. Disappearance of the small-angle x-ray scattering pattern in this region (Fig. 6) is considered as evidence for the absence of the lamellar periodicity.

The general trend of the change in T_{m2} of samples 2 and 3 (Fig. 7) is similar to that of sample 1 in Figure 4. However, it can be noted that T_{m2} of sample 2 is fairly lower than that of sample 1 or 3 due to the lower stretching temperature of sample 2 in comparison with the other two.

The change in density during the stretching is shown in Figure 8. It can be clearly seen that the density decreases gradually when $v_A < 10$, and then rapidly after $v_A = 10$. The tendency is the same for the three samples. The rapid drop in density in region 3 well supports the previously suggested view that biaxial stretching in one step is attained by the pulling out of the chain molecules in lamellae as well as splitting of intermolecular crystals now developed into more slender crystals because amorphous chains yield at the same time by the unfolding of the chain molecules in the lamellae and splitting of intermolecular crystals now developed into more slender crystals. The decrease in density is a striking feature of biaxial stretching

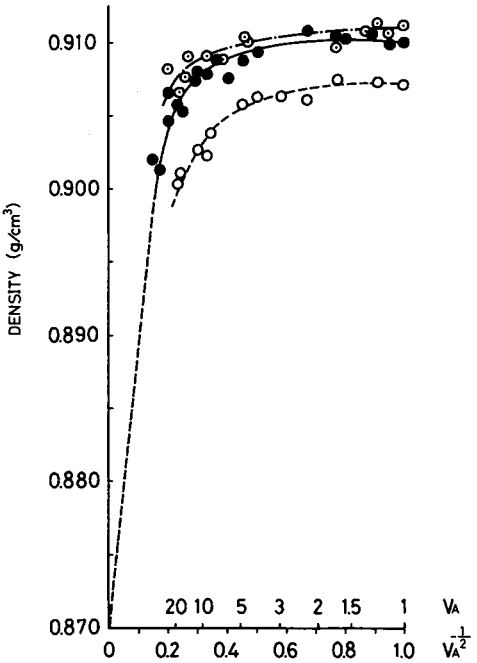

Fig. 8. Change in density during the stretching: (●) sample 1; (○) sample 2; (⊙) sample 3.

in one step in contrast with uniaxial stretching which accelerates crystallization in line with orientation. The photographs of the edge view in Figure 6 show the center streak scattering on the equator. However, the streak cannot necessarily be connected directly with the formation of voids.[29] It is shown qualitatively that the line broadening of the wide-angle x-ray scattering pattern becomes prominent for $v_A > 10$, implying the diminution of crystallite size.[30]

It is noted that the extrapolation of these plots to $v_A^{-1/2} = 0$ attains 0.870 g/cm³ without difficulty, which has been reported as the amorphous density of isotactic polypropylene by Farrow.[24] If this were true, the

structure of the sample should be a planar network composed of the extended chain molecules at infinite v_A. However, this suggestion is open to question because of the slight change in ΔH within the experimental range of v_A, as mentioned below. In order to ascertain this suggestion, samples having v_A larger than 50 are necessary, which, however, cannot be obtained at present because of experimental difficulties.

The change in ΔH is shown in Figure 9. The ΔH value decreases slightly with increase in v_A; and among the three samples, sample 2 gives the smallest value, the other two giving nearly equal ΔH. As mentioned before, the density decreases rapidly when v_A exceeds 10 (Fig. 8), while ΔH does not show such a rapid drop in the corresponding region (Fig. 9). If ΔH is only a function of crystallinity, the changes in density and ΔH should

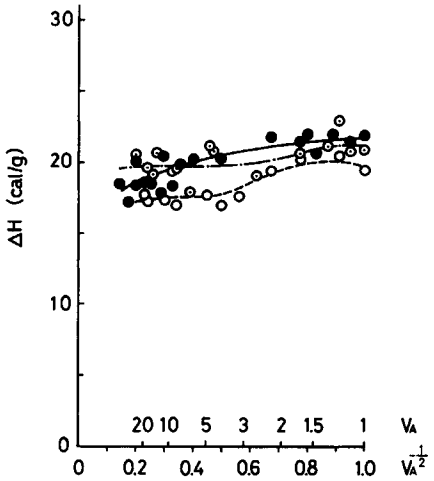

Fig. 9. Plot of ΔH vs. $v_A^{-1/2}$: (●) sample 1; (○) sample 2; (⊙) sample. 3.

correspond with each other. The results shown in Figures 8 and 9 indicate that ΔH is not only a function of crystallinity, but also of the energy level of the amorphous region and crystallite surface. In this case, the effect of the latter seems to play an important role. As the energy level of the fold surface of a crystallite is higher than that of the amorphous region, a fold-type crystal contains rather higher energy in itself and so requires a relatively smaller quantity of energy in the process of melting. On the other hand, an intermolecular crystal, mainly yielded at $v_A > 10$, does not have such a surface energy effect, and thus ΔH is practically unchanged at $v_A > 10$, in spite of the rapid decrease in density.

The authors wish to thank Dr. Masahide Yazawa of the Polymer Processing Research Institute for financial support. They are also grateful to Dr. Hisaaki Kanetsuna of the Research Institute for Polymers and Textiles for helping in the DSC measurement of the samples.

References

1. H. W. Wyckoff, *J. Polym. Sci.*, **62**, 83 (1962).
2. F. Danusso and G. Gianotti, *Makromol. Chem.*, **80**, 1 (1964).
3. W. R. Krigbaum and I. Uematsu, *J. Polym. Sci.*, **3**, 767 (1965).
4. K. Takamizawa, T. Oyama, and Y. Urabe, *Rep. Progr. Polym. Phys. Japan.* **9**, 277 (1966).
5. Y. Abe, T. Yubayashi, H. Sato, and N. Yamada, *Rep. Progr. Polym. Phys. Japan*, **10**, 189 (1967).
6. K. Kamide, *Kobunshi Kagaku*, **25**, 532 (1968).
7. K. Maeda and H. Kanetsuna, *Kogyo Kagaku Zasshi*, **73**, 1413 (1970).
8. J. R. Schaefgen, *J. Polym. Sci.*, **38**, 549 (1959).
9. R. W. Wilkinson and M. Dole, *J. Polym. Sci.*, **58**, 1089 (1962).
10. O. Ishizuka, *Kogyo Kagaku Zasshi*, **65**, 244 (1962).
11. E. Passaglia and H. K. Kevorkian, *J. Appl. Phys.*, **34**, 90 (1963).
12. I. Kirshenbaum, Z. W. Wilchinsky, and B. Groten, *J. Appl. Palym. Sci.*, **8**, 2723 (1964).
13. K. Kamide and K. Nakamura, *Sen-i Gakkaishi*, **24**, 486 (1968).
14. G. Farrow, *Polymer*, **4**, 191 (1963).
15. K. Kamide and M. Sanada, *Kobunshi Kagaku*, **24**, 662 (1967).
16. K. D. Pae and J. A. Sauer, *J. Appl. Polym. Sci.*, **12**, 1901 (1968).
17. J. A. Sauer and K. D. Pae, *J. Appl. Polym. Sci.*, **12**, 1921 (1968).
18. K. Maeda and H. Kanetsuna, *Kogyo Kagaku Zasshi*, **73**, 1407 (1970).
19. R. F. Schwenker and R. K. Zuccarello, *J. Polym. Sci. C*, **No. 6**, 1 (1964).
20. K. Maeda and H. Kanetsuna, *Kogyo Kagaku Zasshi*, **69**, 1789 (1966).
21. H. Shii and K. Ishikawa, *Kobunshi Kagaku*, **27**, 519 (1970).
22. H. Tanaka, T. Masuko, and S. Okajima, *J. Polym. Sci. A-1*, **7**, 3351 (1969).
23. J. B. Kinsinger and R. E. Hughes, *J. Phys. Chem.*, **63**, 2002 (1959).
24. G. Farrow, *Polymer*, **2**, 409 (1961).
25. S. Okajima, K. Kurihara, and K. Homma, *J. Appl. Polym. Sci.*, **11**, 1703 (1967).
26. S. Okajima and T. Masuko, *Sen-i Gakkaishi*, **26**, 438 (1970).
27. T. Masuko, H. Tanaka, and S. Okajima, *J. Polym. Sci. A-2*, **8**, 1565 (1970).
28. H. Tanaka, T. Masuko, K. Homma, and S. Okajilma, *J. Polym. Sci.*, **7**, 1997 (1969).
29. Y. Udagawa, H. Tanaka, and S. Okajima, paper presented at Meeting of the Society of Fibre Science and Technology, Tokyo. Japan, May 1972.
30. H. Tanaka and S. Okajima, in preparation.

Received May 25, 1972
Revised October 17, 1972